Cell Host & Microbe
Article

Selective Subversion of Autophagy Complexes Facilitates Completion of the *Brucella* Intracellular Cycle

Tregei Starr,[1] Robert Child,[1] Tara D. Wehrly,[1] Bryan Hansen,[2] Seungmin Hwang,[3,4] Carlos López-Otin,[5] Herbert W. Virgin,[3,4] and Jean Celli[1,*]
[1]Laboratory of Intracellular Parasites
[2]Electron Microscopy Unit, Research Technologies Branch
Rocky Mountain Laboratories, National Institute of Allergy and Infectious Diseases, National Institutes of Health, Hamilton, MT 59840, USA
[3]Department of Pathology and Immunology
[4]Midwest Regional Center of Excellence for Biodefense and Emerging Infectious Diseases Research
Washington University School of Medicine, St. Louis, MO 63110, USA
[5]Departamento de Bioquímica y Biología Molecular, Facultad de Medicina, Instituto Universitario de Oncología, Universidad de Oviedo, 33006 Oviedo, Spain
*Correspondence: jcelli@niaid.nih.gov
DOI 10.1016/j.chom.2011.12.002

SUMMARY

Autophagy is a cellular degradation process that can capture and eliminate intracellular microbes by delivering them to lysosomes for destruction. However, pathogens have evolved mechanisms to subvert this process. The intracellular bacterium *Brucella abortus* ensures its survival by forming the *Brucella*-containing vacuole (BCV), which traffics from the endocytic compartment to the endoplasmic reticulum (ER), where the bacterium proliferates. We show that *Brucella* replication in the ER is followed by BCV conversion into a compartment with autophagic features (aBCV). While *Brucella* trafficking to the ER was unaffected in autophagy-deficient cells, aBCV formation required the autophagy-initiation proteins ULK1, Beclin 1, and ATG14L and PI3-kinase activity. However, aBCV formation was independent of the autophagy-elongation proteins ATG5, ATG16L1, ATG4B, ATG7, and LC3B. Furthermore, aBCVs were required to complete the intracellular *Brucella* lifecycle and for cell-to-cell spreading, demonstrating that *Brucella* selectively co-opts autophagy-initiation complexes to subvert host clearance and promote infection.

INTRODUCTION

Pathogenic microbes with an intracellular lifestyle have evolved various survival strategies to avoid microbicidal mechanisms and generate unique intracellular niches for replication and persistence, by modulating cellular processes. Intracellular parasites or bacteria typically reside either within a membrane-bound vacuole, which they modify through controlled maturation of their original phagosome or freely in the cytosol after phagosomal escape. Regardless of their intracellular location, invading microorganisms can be recognized as foreign and engaged by macroautophagy (herein referred to as autophagy), an intracellular process of capture and lysosomal degradation of damaged organelles, protein aggregates, and cytosolic content with a prominent role in intracellular innate immunity (Levine et al., 2011). Selective antibacterial autophagy, also called xenophagy, can either target cytosolic bacteria (Checroun et al., 2006; Collins et al., 2009; Nakagawa et al., 2004; Ogawa et al., 2005; Rich et al., 2003) or bacteria in both intact and damaged vacuolar compartments (Birmingham et al., 2006; Gutierrez et al., 2004) and deliver them to lysosomes, thereby controlling their intracellular survival and replication.

Autophagy is initiated by the nucleation of an isolation membrane that elongates to envelop autophagic targets into a double-membrane vacuole, the autophagosome, which in turn progressively matures and eventually fuses with lysosomes to create a degradative autolysosome (Levine et al., 2011). The membrane dynamics of the autophagic process involve various protein complexes required for nucleation and elongation of the autophagosome. Key to the initiation of autophagy is the ULK1 complex, which translocates to subdomains of the endoplasmic reticulum (ER), where it recruits a class III phosphatidylinositol-3-kinase (PI3-kinase) complex comprised of the autophagy proteins VPS34, VPS15, Beclin 1, and Atg14L (Itakura and Mizushima, 2010; Matsunaga et al., 2010; Matsunaga et al., 2009), which in turn generates phosphatidylinositol-3-phosphate (PI3P) on omegasomes (Axe et al., 2008) that serve as cradles for the biogenesis of isolation membranes. Elongation of the isolation membrane into an autophagosome involves two ubiquitin-like conjugation pathways, both dependent on the autophagy protein ATG7, which in aggregate generate the ATG12-ATG5/ATG16L1 protein complex and phosphatidylethanolamine (PE)-conjugated ATG8 homolog LC3 (He and Klionsky, 2009). Given the essential roles of these autophagy protein complexes, depletion of these proteins typically abrogates or severely impairs autophagy, xenophagic control of intracellular microorganisms (Birmingham et al., 2006; Levine et al., 2011; Zheng et al., 2009), and resistance to infection (Zhao et al., 2008), although some ATG5- and ATG7-independent macroautophagic and

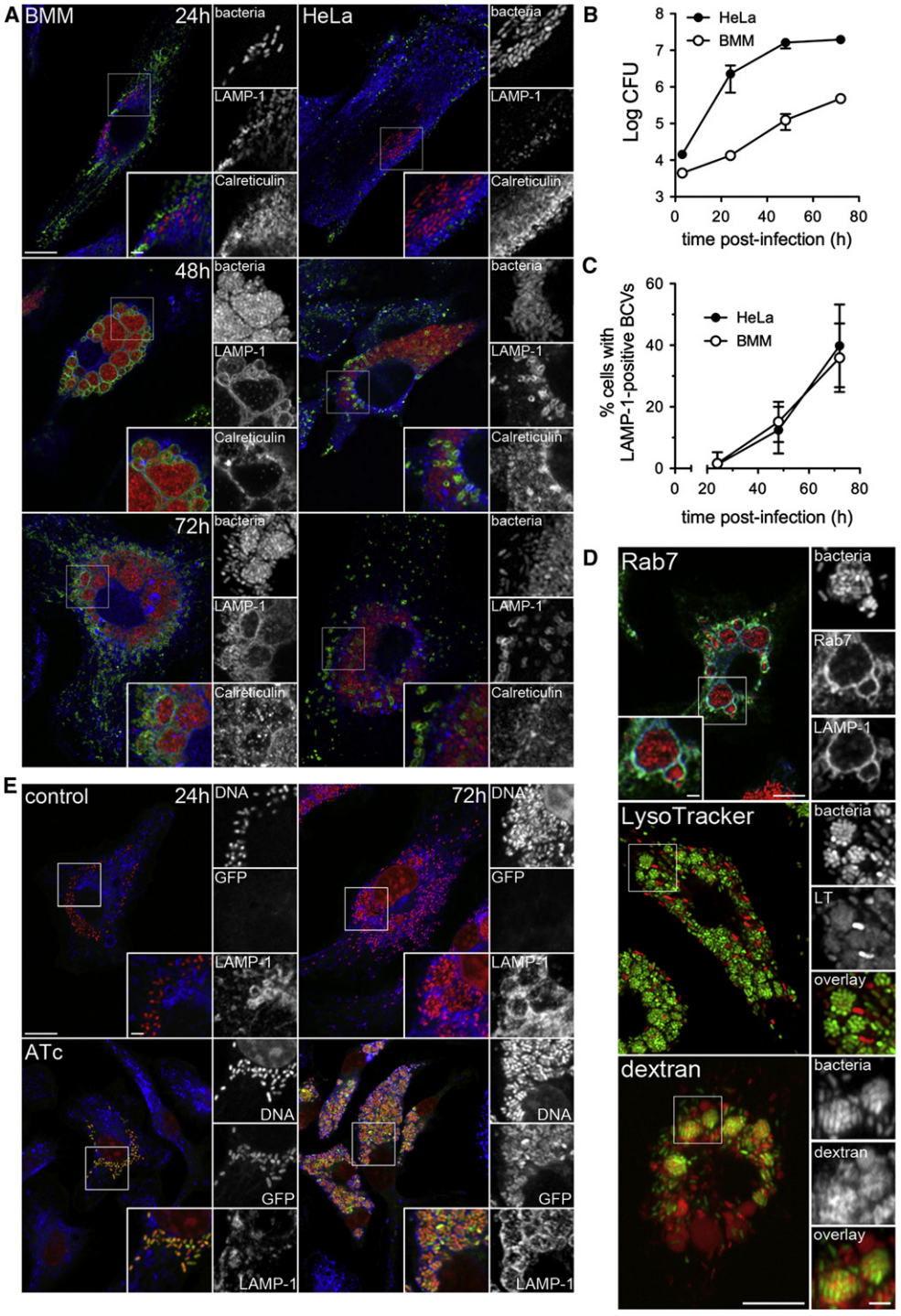

Figure 1. Post-ER Replication Translocation of *Brucella* into an Endosomal Compartment

(A) Representative confocal micrographs of BMMs (left) and HeLa cells (right) infected with $DsRed_m$-expressing *B. abortus* 2308 (red) and immunostained for LAMP-1 (green) and calreticulin (blue) at 24, 48, and 72 hr pi. Scale bars represent 10 and 2 μm.

(B) Intracellular growth of *B. abortus* strain 2308 in either BMMs (open circles) or HeLa cells (closed circles). Cells were infected and intracellular CFUs enumerated at 3, 24, 48, and 72 hr pi. Data are shown as means ± SEM from a representative experiment performed in triplicate.

(C) Quantification of late LAMP-1-positive BCV formation at 24, 48, and 72 hr pi in BMMs (open circles) and HeLa cells (closed circles). Data are expressed as percentage of infected cells containing late LAMP-1-positive BCV and are means ± SD from three independent experiments.

(D) Representative confocal micrographs of BMMs infected with either $DsRed_m$-expressing (Rab7 panel) or GFP-expressing (LysoTracker and dextran panels) *B. abortus* 2308 and processed for labeling of Rab7 and LAMP-1 (Rab7), acidic compartments (LysoTracker), or endocytic compartments (dextran). Scale bars represent 10 and 2 μm.

xenophagic processes have been reported (Collins et al., 2009; Nishida et al., 2009). Due to its prominent antimicrobial functions, various intracellular pathogens have evolved to protect themselves against xenophagic capture, including the cytosolic bacteria *Listeria monocytogenes* (Birmingham et al., 2007; Yoshikawa et al., 2009) and *Shigella flexneri* (Ogawa et al., 2005). Additionally, general autophagy has been invoked in the intracellular trafficking of the vacuolar bacteria *Coxiella burnetii* (Gutierrez et al., 2005), *Yersinia pestis* and *pseudotuberculosis* (Moreau et al., 2010; Pujol et al., 2009), *Porphyromonas gingivalis* (Dorn et al., 2001), and *Brucella abortus* (Pizarro-Cerdá et al., 1998a).

Bacteria of the genus *Brucella* are the causative agent of brucellosis, a worldwide zoonosis with significant health and economic consequences (Pappas et al., 2005). Essential to the virulence of these bacteria is their ability to enter, survive, proliferate, and persist within a variety of host cell types, including professional phagocytes such as macrophages and dendritic cells (Archambaud et al., 2010; Salcedo et al., 2008). *Brucella* has evolved to manipulate intracellular membrane trafficking processes to foster its survival and growth. After phagocytic uptake or internalization, *Brucella* resides within a membrane-bound compartment, the *Brucella*-containing vacuole (BCV), which traffics along the endocytic pathway during the first 8 hr postinfection (pi) and undergoes limited fusion with the lysosomal compartment (Starr et al., 2008). These interactions with late-endocytic/lysosomal compartments are necessary for induction of the VirB type IV secretion apparatus (Boschiroli et al., 2002; Starr et al., 2008), a major virulence factor that translocates effector molecules into the host cell (de Jong et al., 2008; Marchesini et al., 2011) and probably promotes endosomal BCV (herein referred to as eBCV) trafficking toward the ER (Celli et al., 2003; Comerci et al., 2001). BCV trafficking to the ER occurs via interactions with the transitional ER between 4 and 12 hr pi, which requires the small GTPases Sar1 (Celli et al., 2005) and Rab2 (Fugier et al., 2009) and culminates in endosomal to ER membrane exchange on the BCV (Celli et al., 2003). ER-derived BCVs are replication-permissive organelles (herein referred to as rBCVs) that are generated by 12 hr pi (Celli et al., 2003; Comerci et al., 2001; Pizarro-Cerdá et al., 1998a; Salcedo et al., 2008). *Brucella* replication also requires the ER transmembrane protein IRE1α (Qin et al., 2008), a sensor of the unfolded protein response (UPR) upon ER stress that also contributes to autophagy induction (Ogata et al., 2006).

While the *Brucella* intracellular cycle is well defined from entry to replication in the ER, with initial rounds of replication achieved within 12 to 24 hr pi (Arellano-Reynoso et al., 2005; Bellaire et al., 2005; Celli et al., 2003, 2005; Comerci et al., 2001; Fugier et al., 2009; Pizarro-Cerdá et al., 1998b; Salcedo et al., 2008), steps subsequent to bacterial replication in rBCVs are unknown. Here, we have examined late stages of the *Brucella* intracellular cycle in both macrophages and epitheloid cells. We report a post-ER replication compartment that is initiated at the ER and converts rBCVs into vacuoles with autophagic features in a Beclin1-, ULK-1-, and ATG14L-dependent but ATG5-, ATG16L1-, ATG4B-, ATG7-, and LC3B-independent manner. Importantly, rBCV conversion into these vacuoles completes the intracellular cycle of *Brucella* and promotes cell-to-cell spread. These findings demonstrate a selective subversion of autophagy nucleation complexes by a pathogenic bacterium in favor of an infection process.

RESULTS

Brucella Translocates into Endosomal Vacuoles at Late Stages of Its Intracellular Cycle

To examine late stages of the *Brucella* intracellular cycle, we first monitored intracellular growth of the virulent wild-type *B. abortus* strain 2308 in either C57BL/6J murine bone marrow-derived macrophages (BMMs) or in the human epithelioid cell line HeLa. Increasing numbers of viable intracellular bacteria were recovered during a 72 hr infection period, demonstrating bacterial replication in both cell types (Figure 1B). Confocal immunofluorescence microscopy analysis revealed *Brucella* already recognized replication patterns within LAMP-1-negative, Calreticulin-positive rBCVs at 24 hr pi (Figure 1A), indicating that internalized bacteria had generated ER-derived replicative organelles (rBCVs) at this stage. At 48 hr pi, most infected cells bore increasing numbers of ER-localized, replicating bacteria. However, 15% ± 6.5% of infected BMMs contained clusters of bacteria enclosed within large LAMP-1-positive vacuoles, and 12% ± 7.6% of infected HeLa cells harbored LAMP-1-positive vacuoles containing either one or more bacteria embedded within, or at the periphery, of rBCV clusters (Figures 1A and 1C). This compartment was more prevalent by 72 hr pi, where 36% ± 11% and 40% ± 13% of infected BMMs and HeLa cells contained LAMP-1-positive, calreticulin-negative vacuoles (Figures 1A and 1C), suggesting that replicating *Brucella* translocate to a vacuolar compartment that is phenotypically distinct from ER-derived rBCVs.

Consistently, these late BCVs recruited the late endosomal/lysosomal GTPase Rab7, were acidified and accumulated fluid phase markers in BMMs (Figure 1D), demonstrating their fusogenocity with late endocytic compartments. To verify that these large endosomal vacuoles harbored live bacteria, BMMs were infected with *B. abortus* 2308 expressing GFP under an anhydrotetracycline (ATc)-inducible promoter and examined for bacterial fluorescence upon induction. Like bacteria within either eBCVs (8h pi; data not shown) or rBCVs (24 hr pi; Figure 1E), those contained within LAMP-1-positive vacuoles at 72 hr pi expressed GFP upon ATc treatment once these vacuoles were formed (Figure 1E), demonstrating that they are transcriptionally active, in agreement with the sustained recovery of viable bacteria after 48 hr pi (Figure 1B).

Controlling secondary infections with a low concentration of gentamicin (25 μg/ml) from 24 hr pi onward did not affect the formation of this compartment (Figures S1A and S1B available online). Therefore these late endosomal vacuoles do not originate from reinfection events and constitute a post-ER replication

(E) Representative confocal micrographs of BMMs infected with *B. abortus* 2308 expressing an anhydrotetracycline (ATc)-inducible GFP that were left untreated or treated for 6 hr with 200 nM ATc prior to processing at 24 and 72 hr pi for bacterial and host-cell DNA (red) and LAMP-1 (blue) labeling. Scale bars represent 10 and 2 μm.
See also Figure S1.

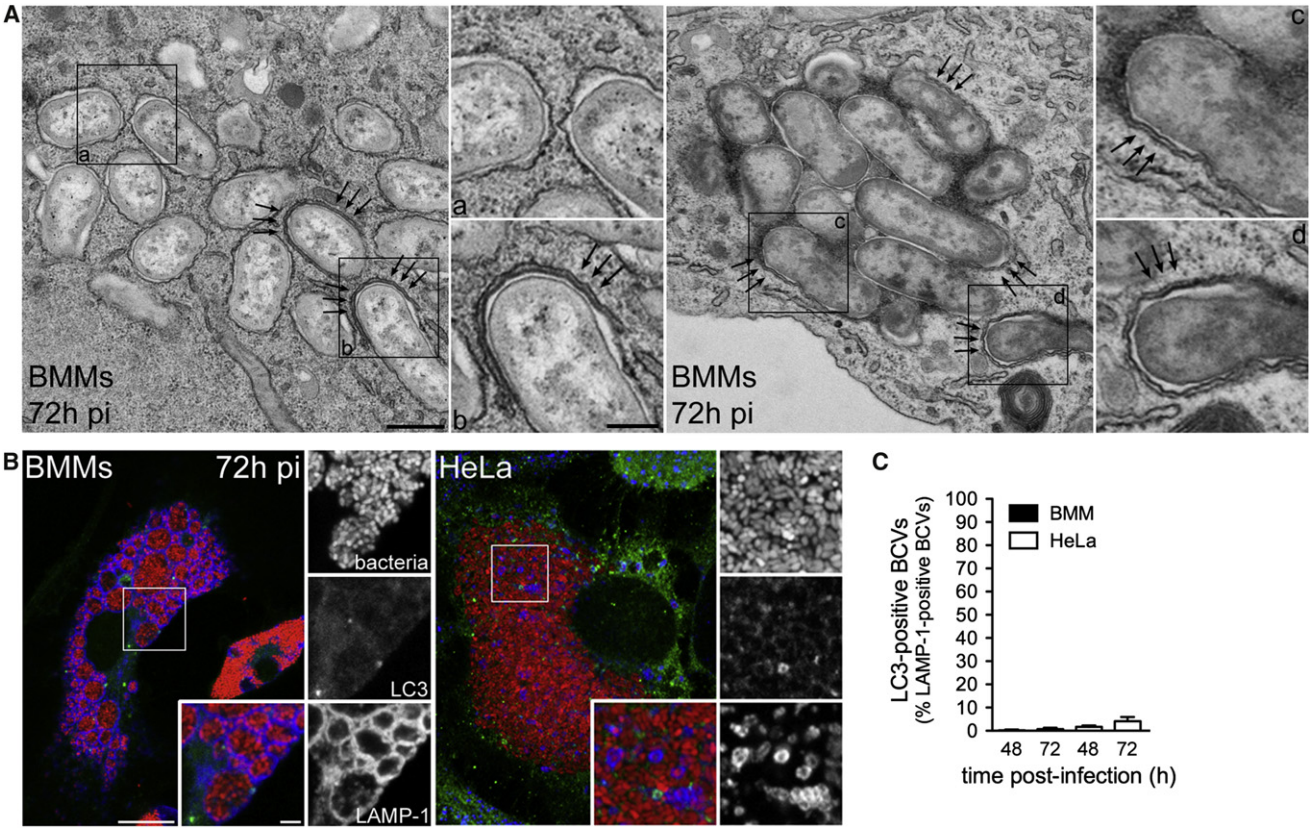

Figure 2. Late Endosomal BCVs Display Structural Features of Autophagy, but Do Not Accumulate the Autophagy protein LC3

(A) Representative TEM images of BMMs infected with *B. abortus* 2308 for 72 hr. Arrows indicate double-membrane structures on BCVs or wrapping around single membrane BCVs. Inset a shows single-membrane rBCVs. Insets b, c, and d show multimembrane BCVs. Scale bars represent 500 and 200 nm.

(B) Representative confocal micrographs of BMMs (left) or HeLa cells (right) infected with $DsRed_m$-expressing *B. abortus* 2308 (red) and immunostained for LC3 (green) and LAMP-1 (blue) at 72 hr pi. Scale bars represent 10 μm and 2 μm.

(C) Quantification of late LAMP-1-positive BCVs that accumulated LC3 at 48 and 72 hr pi in BMMs (filled bars) and HeLa cells (open bars). Data are shown as means ± SD from three independent experiments.

See also Figure S2.

stage of the bacterium's intracellular cycle. Ultrastructural analysis of these vacuoles revealed that, unlike rBCVs that typically display single, ribosome-laden membranes, (Figure 2A, inset a) (Celli et al., 2003)), ~20% of BCVs at 72 hr pi in BMMs (Figure 4A) were either engulfed by double-membrane crescents (Figure 2A, inset b) or delimited by multiple membranes (Figure 2A, inset d, and Figure 4A), suggestive of an autophagy process. Double membrane-bound bacterial clusters consistent with large vacuoles (Figure 1A) were also detected (Figure 2A, inset c, and Figure S2) and their endosomal nature was confirmed by immunoelectron microscopy in both BMMs and HeLa cells (72 hr pi; Figure S2B). Taken together, these observations indicate that after ER replication, endosomal BCVs display structural features consistent with an autophagic process and were named autophagic BCVs, or aBCVs.

aBCV Formation Requires the Autophagy-Associated Proteins Beclin1 and ULK1

Given the ultrastructural features of aBCVs, we next examined whether these vacuoles display markers of autophagic membranes. Using LAMP-1 as a marker for aBCVs, we did not detect endogenous LC3 isoforms on these vacuoles in either BMMs or HeLa cells at 48 or 72 hr pi (Figures 2B and 2C), indicating that their membranes did not accumulate LC3. Despite these results, we examined the potential role of various autophagy proteins in aBCV formation via small interfering RNA (siRNA)-mediated depletion in HeLa cells and first tested whether their depletion affected *Brucella* trafficking to the ER. Based on LAMP-1 exclusion during biogenesis of rBCVs (Celli et al., 2003; Comerci et al., 2001; Salcedo et al., 2008; Starr et al., 2008), single depletions of either the autophagy-elongation proteins ATG5, ATG7, LC3B, or the autophagy-initiation proteins Beclin1 or ULK1 (Figure S3A) did not affect eBCV maturation into rBCVs (Figure 3A), although they did prevent rapamycin-induced LC3 lipid conjugation (Figure S3B). This demonstrates that a functional autophagy pathway is not required for *Brucella* trafficking to the ER. Depletion of either ULK1 or Beclin 1 significantly decreased formation of aBCVs at 48 and 72 hr pi, and their combined depletion nearly abolished aBCV formation (Figure 3B; $p < 0.05$), despite unaffected intracellular bacterial proliferation (Figures 3D and 3E). This indicates that aBCV formation requires functional ULK1 and Beclin 1 autophagy-initiation/nucleation

complexes and is unrelated to bacterial replication. By contrast, knockdown of ATG5, ATG7, or LC3B did not impair, but instead potentiated, aBCV formation (Figure 3C; $p < 0.05$), indicating that, consistent with the lack of LC3 recruitment to aBCVs (Figures 2B and 2C), canonical autophagy-elongation complexes are not involved in aBCV formation. To confirm these findings in macrophages, we depleted either Atg7 or Beclin 1 (Figures 3F–3H) and examined aBCV formation at 72 hr pi. Compared to a nontargeting (siNT) control, Atg7 depletion did not affect aBCV formation (Figures 3G and 3H), yet Beclin 1 depletion significantly reduced this process (Figures 3G and 3H). Hence, aBCV formation in macrophages also requires the autophagy nucleation protein Beclin 1, but not the autophagy-elongation protein Atg7.

aBCV Formation Is Independent of Autophagy-Elongation Complexes

To exclude the possibility that the ATG5, ATG7, or LC3B independence of aBCV formation results from residual activity due to incomplete siRNA-mediated depletion, we examined aBCV formation in various autophagy null mutation BMMs. Using either *Atg5*$^{flox/flox}$ control mice or *Atg5*$^{flox/flox}$*-Lyz-Cre* mice lacking Atg5, *Atg16L1*$^{flox/flox}$ control mice or *Atg16L1*$^{flox/flox}$*-Lyz-Cre* mice lacking Atg16L1 or *Atg4B*$^{-/-}$ mice, we first tested whether the absence of these proteins affected *Brucella* trafficking to the ER. Consistent with our results in HeLa cells, the timing and extent of eBCV to rBCV maturation was indistinguishable in either control C57BL/6J, *Atg5*$^{flox/flox}$ control or *Atg5*$^{flox/flox}$*-Lyz-Cre* BMMs (Figures S4A and S4B), demonstrating that *Brucella* trafficking to the ER is independent of Atg5. Similarly, *Brucella* trafficking to the ER was unaffected in either *Atg16L1*$^{flox/flox}$ control *Atg16L1*$^{flox/flox}$*-Lyz-Cre* or *Atg4B*$^{-/-}$ BMMs (Figure S4C), confirming that *Brucella* trafficking to the ER is independent of these autophagy proteins. Biogenesis of aBCVs was also not impaired in the absence of either Atg5, Atg16L1, or Atg4B (Figures 4A and 4B), since aBCVs formed similarly in either control (C57BL6/J, *Atg5*$^{flox/flox}$, *Atg16L1*$^{flox/flox}$) or deficient (*Atg5*$^{flox/flox}$*-Lyz-Cre*, *Atg16L1*$^{flox/flox}$*-Lyz-Cre*, *Atg4B*$^{-/-}$) BMMs, and was even slightly more pronounced in the null mutation BMMs (Figure 4B). Furthermore, ultrastructural analysis of aBCVs in *Atg5*$^{flox/flox}$*-Lyz-Cre*, *Atg16L1*$^{flox/flox}$*-Lyz-Cre* and *Atg4B*$^{-/-}$ BMMs showed aBCVs with closed double or multimembranes at frequencies comparable to control BMMs (Figure 4A). Complete formation of aBCVs in the absence of these autophagy-elongation proteins in BMMs demonstrates that aBCV formation is an Atg5-, Atg16L1-, and Atg4B-independent process.

Altogether, aBCV formation in both macrophages and epithelioid cells depends upon the autophagy-associated proteins Beclin 1 and ULK1 but not the autophagy-elongation proteins ATG5, ATG16L1, ATG7, ATG4B, and LC3B.

ER-Localized Beclin 1-ATG14L Complexes Are Required for aBCV Formation

Three Beclin 1-PI3-kinase complexes have been identified that are compartmentalized and fulfill differential functions through their association with the additional subunits ATG14L/Barkor, Rubicon, and UVRAG (Itakura et al., 2008; Liang et al., 2008; Matsunaga et al., 2009; Sun et al., 2008). The ATG14L-containing complex localizes to the ER and is required for autophagy initiation (Axe et al., 2008; Itakura et al., 2008; Itakura and Mizushima, 2010; Matsunaga et al., 2009, 2010), while UVRAG-containing complexes localize to Rab9-positive endocytic compartments and modulate autophagosome maturation and endocytic trafficking (Itakura et al., 2008; Liang et al., 2008; Matsunaga et al., 2009; Thoresen et al., 2010; Zhong et al., 2009). Given the ER nature of rBCVs and the requirement of Beclin 1 for the progression of *Brucella* infection from rBCVs into aBCVs, we tested whether the ER-localized Beclin 1 complex is required for aBCV formation. First, treatment with the class III PI3-kinase inhibitor 3-methyladenine (3-MA) or the PI3-kinase inhibitor LY294002 for 14 hr, reduced aBCV formation by ~50% and 75% in BMMs and HeLa cells, respectively (Figure 5A), indicating that aBCV formation depends upon PI3-kinase activity. Furthermore, aBCVs showed recruitment of a 2xFYVE-GFP fusion protein in HeLa cells (Figure 5B), indicating PI3P generation at sites of aBCV biogenesis. Hence, PI3-kinase activity is detectable at sites of aBCV formation and required for their formation.

We next depleted either ATG14L or UVRAG in HeLa cells (Figure S3) to determine which Beclin 1 complex(es) are involved in aBCV formation. Depletion of ATG14L, which prevents targeting of the Beclin 1-VPS34-VPS15 autophagy complex to the ER (Matsunaga et al., 2010), reduced aBCV formation by ~45% (Figure 5C), similar to the effect of Beclin 1 depletion (Figure 3B). By contrast, depletion of UVRAG did not affect aBCV formation (Figure 5C), indicating that the endocytic trafficking-associated functions of Beclin 1 complexes do not contribute to aBCV formation. Consistently, depletion of Rab9 also did not affect aBCV formation (Figure S5). Altogether, this demonstrates that the ER localized Beclin 1-PI3-kinase complex is engaged on rBCVs to generate aBCVs, functionally linking the biogenesis of these vacuoles to autophagy initiation.

aBCV Formation Completes the *Brucella* Intracellular Cycle and Promotes Subsequent Infections

Given the late occurrence of aBCVs, we tested whether they contribute to completing the bacterium's infectious cycle, by promoting bacterial egress and subsequent infections. Secondary infection events were examined in HeLa cells, in which isolated, infected cells could be monitored for their ability to generate infection foci through subsequent bacterial invasion of neighboring cells. HeLa cells left untreated (data not shown) or treated with nontargeting siRNA (siNT; Figure 6C) showed that 50% ± 2.8% of highly infected cells generated infection foci by 72 hr pi (Figures 6C and 6D), indicating that infected cells release infectious bacteria in their vicinity. Most (78% ± 1.9%) of these infection foci were associated with aBCV-containing cells (Figures 6A and 6B), correlating aBCV formation with reinfection events. Consistent with aBCV biogenesis, the formation of infection foci was significantly reduced upon depletion of Beclin1, ULK1, or both proteins (Figures 6C and 6D), but not upon depletion of ATG5, ATG7, or LC3B (Figure 6D). This indicates that aBCV formation promotes bacterial release and infection of adjacent cells (Figure S6), but does not contribute to bacterial proliferation (Figure 3E). Hence, aBCV formation allows for the completion of the *Brucella* intracellular cycle and promotes cell-to-cell spread.

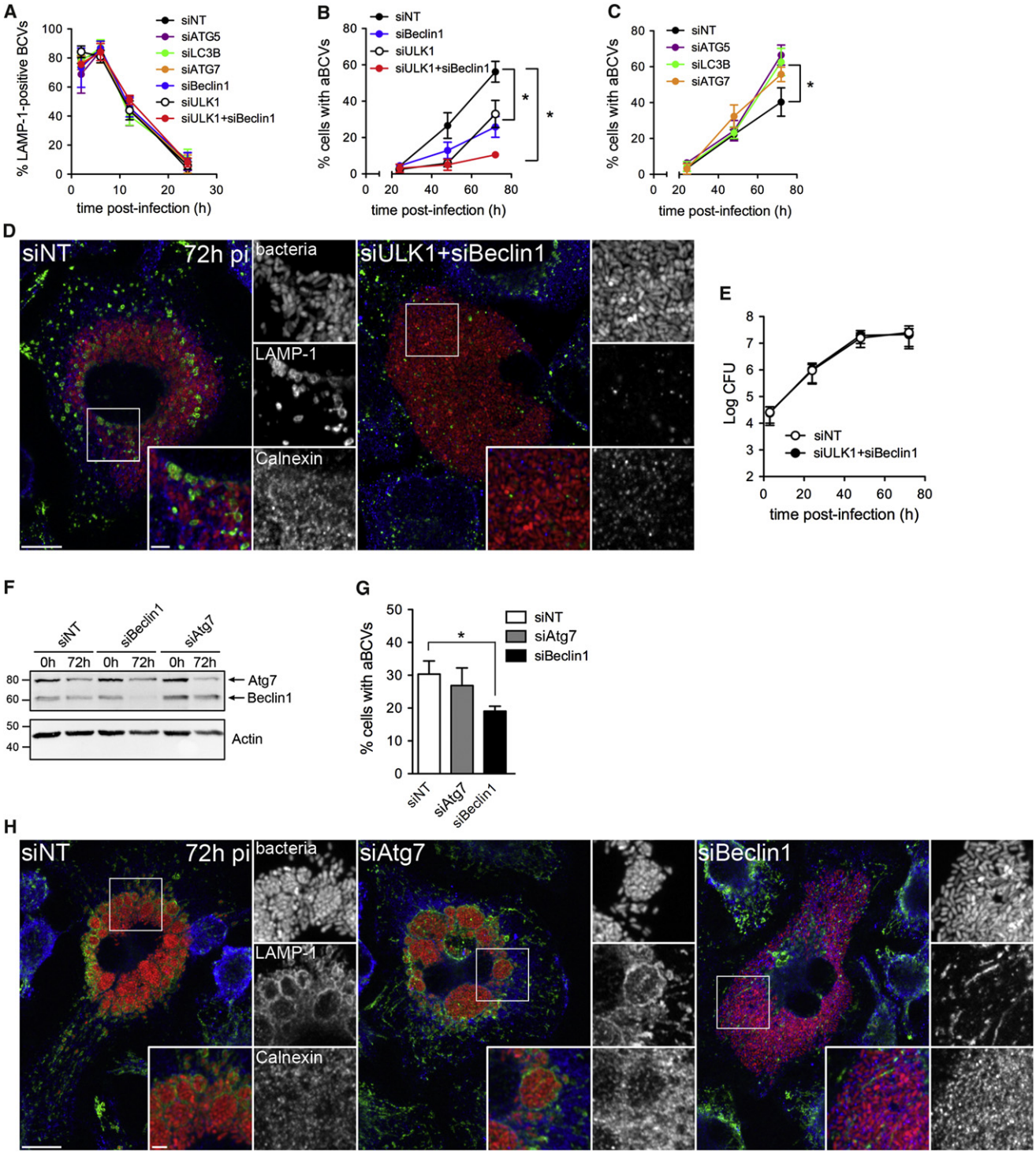

Figure 3. Role of Autophagy Proteins in *Brucella* Trafficking and aBCV Formation

(A) Quantification of LAMP-1-positive BCVs up to 24 hr in siRNA-depleted HeLa cells.

(B) Quantification of aBCV formation at 24, 48, and 72 hr pi in HeLa cells treated with nontargeting siRNA (siNT), siBeclin 1, siULK1, or siULK1 and siBeclin 1.

(C) Quantification of aBCV formation at 24, 48, and 72 hr pi in HeLa cells treated with nontargeting siRNA (siNT), siATG5, siLC3B, or siATG7. All data are shown as means ± SD from three independent experiments.

(D) Representative confocal micrographs of HeLa cells treated with either nontargeting (siNT) or siULK1+siBeclin1 siRNAs, infected with $DsRed_m$-expressing *B. abortus* 2308 (red) and immunostained for LAMP-1 (green) and calnexin (blue) at 72 hr pi. Scale bars represent 10 and 2 μm.

(E) Representative intracellular growth curves of *B. abortus* 2308 in HeLa cells treated with either nontargeting (siNT) or siULK1+siBeclin1 siRNAs. Data are shown as means ± SEM from a representative experiment performed in triplicate.

DISCUSSION

As a prominent player in intracellular innate immunity, autophagy controls the fate of many intracellular microbes (Levine et al., 2011) through xenophagic capture that involves the canonical, ATG protein-dependent nucleation and elongation machineries originally identified as actors of non selective bulk autophagic degradation (Birmingham et al., 2006; Nakagawa et al., 2004; Ogawa et al., 2005). Similarly, bacterial pathogens that may benefit from autophagy, such as *C. burnetii*, *Y. pestis*, and *Y. pseudotuberculosis*, seem to do so by also subverting ATG5- and LC3-dependent processes (Gutierrez et al., 2005; Moreau et al., 2010; Pujol et al., 2009). Hence, interactions of pathogens with autophagy generally invoke ATG5- and LC3-dependent autophagy machineries, with the exception of the ATG5-independent capture of cytosolic *M. marinum* (Collins et al., 2009). Here, we uncover a case of bacterial subversion of ULK1-, Beclin 1-, and ATG14L-dependent, but ATG5-, ATG4B-, ATG16L1-, ATG7-, and LC3B-independent, autophagy-like membrane rearrangements that benefits the infection process of the intracellular pathogen *B. abortus*.

Previous studies of the *Brucella* intracellular cycle in epithelial cells have implicated autophagy in its trafficking to the ER (Pizarro-Cerdá et al., 1998a; Pizarro-Cerdá et al., 1998b). It was recently proposed that the UPR receptor IRE1α promotes *Brucella* intracellular growth by inducing autophagosome formation at the ER, which in turn promotes BCV fusion with this compartment (Qin et al., 2008). Yet, this model awaits experimental confirmation and the initial evidence for autophagy-dependent *Brucella* trafficking (Pizarro-Cerdá et al., 1998a, 1998b) lacked the scrutiny of current methods that specifically interrogate this pathway (Mizushima et al., 2010). By examining *Brucella* trafficking to the ER using either macrophages carrying various null mutations in ATG proteins or HeLa cells depleted of an array of autophagy-associated proteins, we demonstrate here that this bacterium does not require the autophagy proteins ATG5, ATG7, ATG16L1, ATG4B, LC3B, Beclin 1, and ULK1 to generate ER-derived rBCVs, nor does it recruit LC3 on BCVs at any stage (data not shown), clearly ruling out a role for this pathway in *Brucella* trafficking to the ER in both murine and human cells. Instead, we show that that ULK1- and Beclin1-dependent autophagy nucleation machineries contribute to a post-ER replication stage of the *Brucella* life cycle, in which bacteria generate aBCVs to complete their infectious cycle. The formation of endosomal aBCVs from ER-derived rBCVs is reminiscent of the maturation of *Legionella pneumophila*-containing vacuoles into acidic, endocytic organelles (Sturgill-Koszycki and Swanson, 2000), since this bacterium also proliferates within ER-derived vacuoles (Swanson and Isberg, 1995). This suggests that pathogens exploiting the secretory pathway may take advantage of common membrane rearrangements exemplified by aBCV biogenesis to (re-)enter the endosomal compartment and complete their infectious cycle.

The reliance of aBCV formation on nucleation but not elongation complexes indicates that *Brucella* either partially co-opts the canonical autophagic pathway and uses yet to be uncovered membrane rearrangements to complete rBCV to aBCV conversion, or subverts an autophagic process that is independent of the canonical elongation complexes. Interestingly, depletion of ATG5, ATG7, or LC3B enhanced aBCV formation in HeLa cells, as did null mutations in Atg5, Atg16L1, and Atg4B in BMMs, arguing that autophagy-elongation complexes functionally compete with the mechanisms of aBCV formation, possibly along an alternative pathway. Indeed, Nishida et al. recently reported an ATG5/ATG7-independent alternative autophagy-like process that, similarly to aBCV formation, required Beclin 1 and ULK1 and was not associated with LC3 recruitment (Nishida et al., 2009). However, this pathway also depends upon the small GTPase Rab9 (Nishida et al., 2009), yet aBCV formation did not require Rab9 in HeLa cells. Hence, we propose that ER-localized brucellae engage membrane rearrangements dependent upon a subset of autophagy-associated proteins, that may contribute to unconventional xenophagic responses at the ER and possibly other yet to be identified autophagy-related host processes.

The signals that initiate aBCV formation remain to be characterized. Although ER stress can induce autophagy via the UPR (Bernales et al., 2006; Ogata et al., 2006), *Brucella* infection was not associated with induction of the UPR (data not shown), suggesting this pathway is not triggered upon *Brucella* proliferation in the ER, or is bacterially inhibited, and probably does not account for aBCV formation. It remains to be determined whether the requirement for ULK1 in aBCV formation links this process to nutrient availability via mTOR (Levine et al., 2011), or whether the ULK1 complex is activated upon different, infection-related signals and detection of pathogen-associated molecular patterns (PAMPs). The strong association of aBCVs with infection foci indicates that these late vacuoles contribute to bacterial release, either by promoting an exocytic process or through cell death and bacterial egress. While the hypothesis of an exocytic egress requires additional investigation, we did not detect any significant cell death in the *Brucella* infected cell populations concomitant with aBCV formation (data not shown), consistent with the reported ability of *Brucella* to prevent programmed cell death in monocytes and epithelial cells (Ferrero et al., 2009; Gross et al., 2000). While future studies should clarify the mechanisms of bacterial release and reinfection, our findings advance our understanding of *Brucella* intracellular pathogenesis and demonstrate a case of selective subversion of autophagy-associated machineries to the benefit of a bacterial cellular infection process.

(F) Representative western blot analysis of Atg7 and Beclin1 depletion at 0 and 72 hr pi in BMMs treated with nontargeting siRNAs (siNT), siBeclin1, or siATG7. Actin was used as a loading control.

(G) Quantification of aBCV formation at 72 hr pi in BMMs treated with nontargeting siRNAs (siNT), siAtg7, or siBeclin1. Data are shown as means ± SD from three independent experiments.

(H) Representative confocal micrographs of C57BL/6J BMMs treated with nontargeting (siNT), siAtg7, or siBeclin1 siRNAs, infected with $DsRed_m$-expressing *B. abortus* 2308 (red) and immunostained for LAMP-1 (green) and calnexin (blue) at 72 hr pi. Scale bars represent 10 and 2 μm.

Asterisks denote statistically significant differences (two-tailed Student's t test; $p < 0.05$). See also Figure S3.

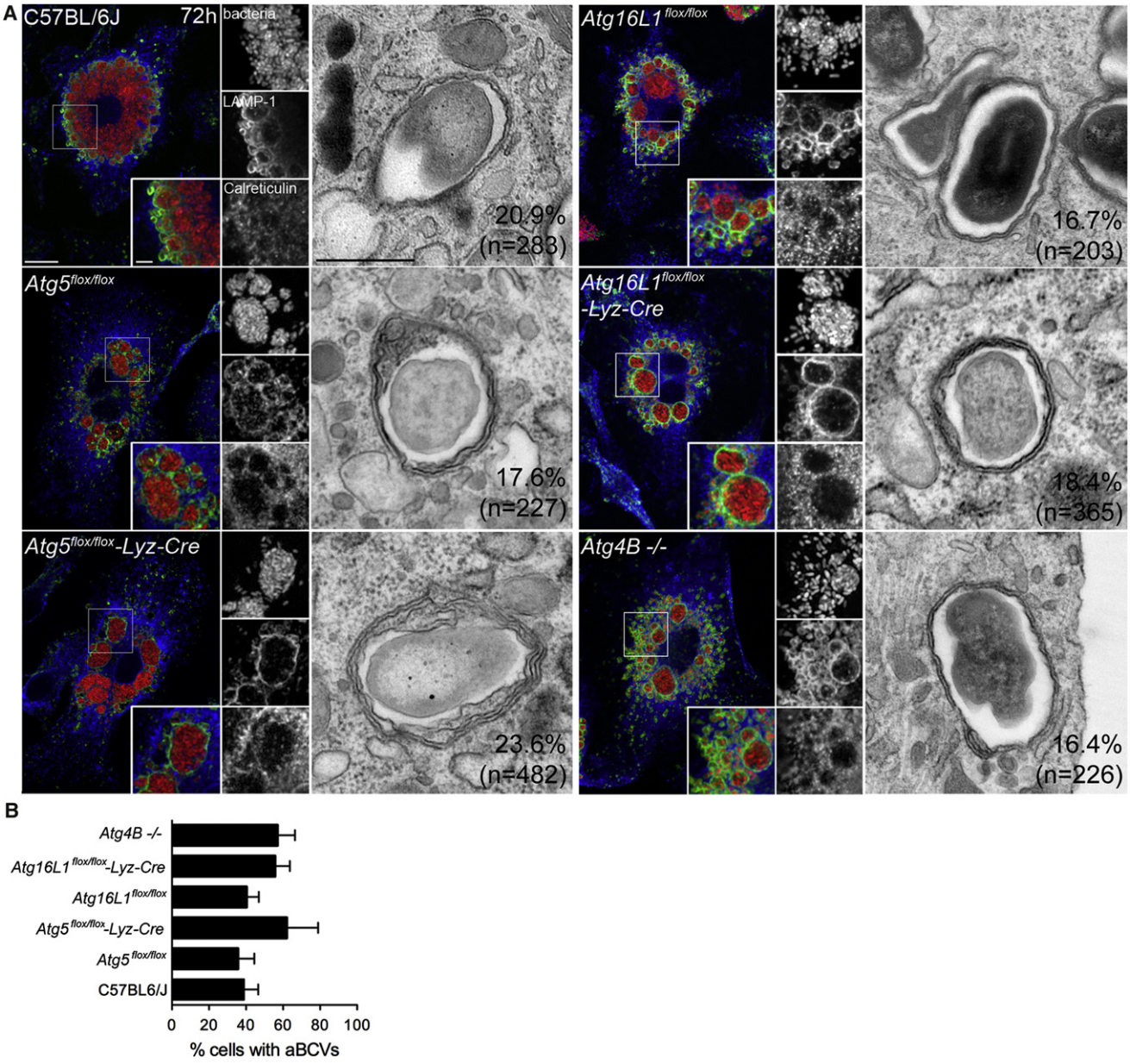

Figure 4. Atg5, Atg16L1, and Atg4B Are Not Required for aBCV Formation

(A) Representative fluorescence confocal and TEM images of C57BL/6J, *Atg5*$^{flox/flox}$, *Atg5*$^{flox/flox}$*-Lyz-Cre*, *Atg16L1*$^{flox/flox}$, *Atg16L1*$^{flox/flox}$*-Lyz-Cre*, and *Atg4B*$^{-/-}$ BMMs infected with either *B. abortus* 2308 (TEM) or DsRed$_m$-expressing *B. abortus* 2308 (red) and immunostained for LAMP-1 (green) and calreticulin (blue) at 72 hr pi. Scale bars represent 10 and 2 μm (immunofluorescence) or 500 nm (TEM). Values on electron micrographs represent the percentage of bacteria contained within multimembrane BCVs and the number of bacteria analyzed from two independent experiments.

(B) Quantification of LAMP-1-positive BCVs (aBCVs) formation in C57BL/6J, *Atg5*$^{flox/flox}$, *Atg5*$^{flox/flox}$*-Lyz-Cre*, *Atg16L1*$^{flox/flox}$, *Atg16L1*$^{flox/flox}$*-Lyz-Cre*, and *Atg4B*$^{-/-}$ BMMs infected with DsRed$_m$-expressing *B. abortus* 2308 for 72 hr. Data are shown as means ± SD from three independent experiments.

See also Figure S4.

EXPERIMENTAL PROCEDURES

Bacterial Strains and Plasmids

The bacterial strains used in this study were the smooth virulent *Brucella abortus* strain 2308 and two derivatives expressing either the monomeric red fluorescent protein DsRed$_m$ from plasmid pJC44 (Starr et al., 2008) or the green fluorescent protein GFP under the control of the tetracycline-inducible promoter *tetA* from *Tn*10 on plasmid pJC45 (see the Supplemental Experimental Procedures). All bacteria were grown in tryptic soy broth (TSB; Sigma) or on TS agar plates (TSA; Sigma) supplemented with kanamycin (50 μg/ml) to select the pBBR1-MCS2 derivatives pJC44 and pJC45. For infection of eukaryotic cells, 2 ml TSB was inoculated with a few bacterial colonies from a freshly streaked TSA plate and grown at 37°C to early stationary phase.

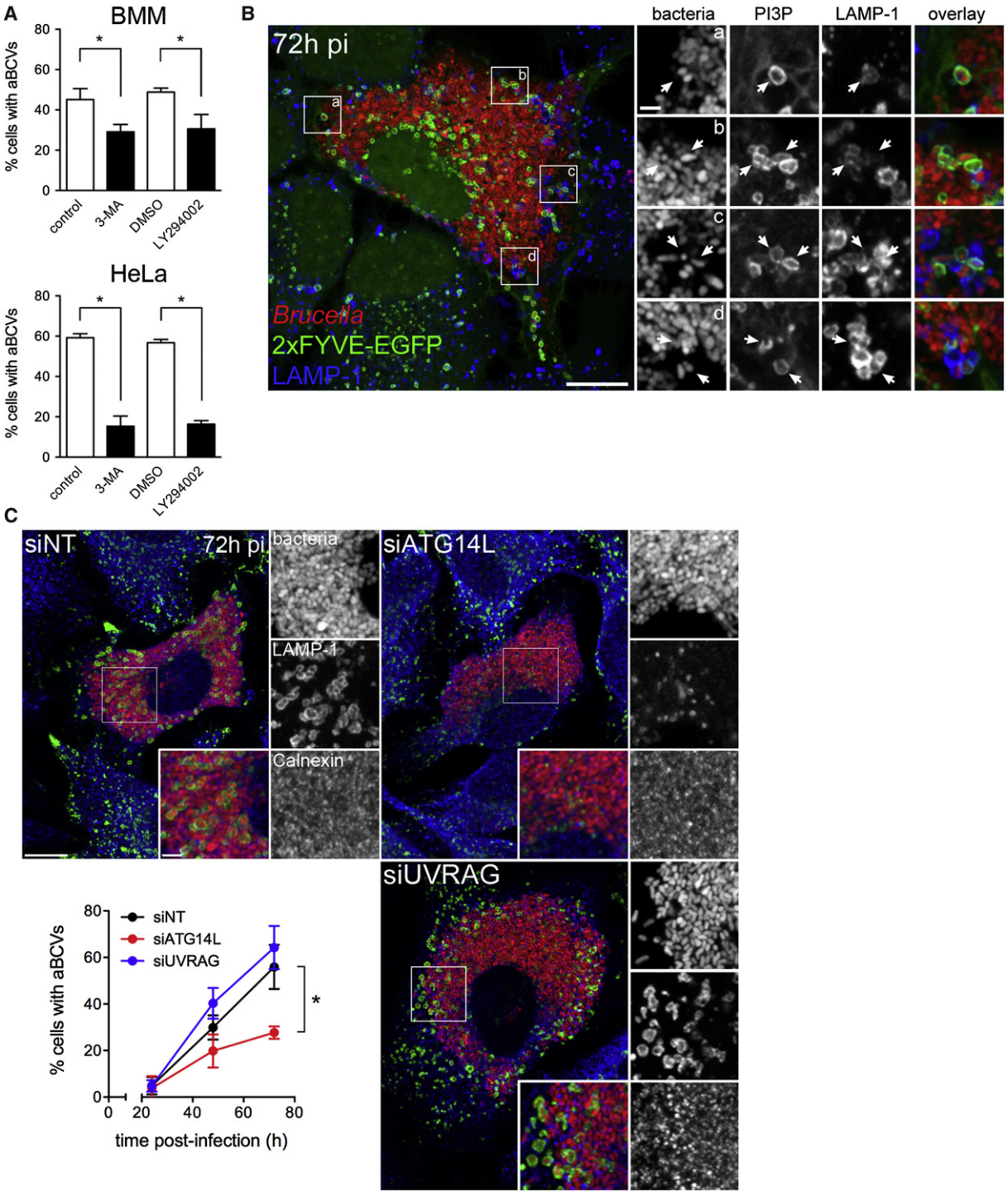

Figure 5. aBCV Formation Requires PI3-Kinase Activity and the Beclin1-ATG14L Complex

(A) Quantification of aBCV formation in either *Brucella*-infected BMMs (top) or HeLa cells (bottom) that were treated with carrier controls (H_2O or DMSO), 3-MA (10 mM), or LY294002 (50 μM) for 14 hr prior to analysis at 72 hr pi. Data are shown as means ± SD from three independent experiments.

(B) Representative confocal micrograph of a HeLa cell expressing the PI3P probe, 2xFYVE-GFP (green), that was infected with $DsRed_m$-expressing *B. abortus* 2308 (red) for 72 hr pi and processed for LAMP-1 immunostaining (blue). Insets are magnifications of the boxed areas on the main image. Scale bars represent 10 and 2 μm.

(C) Representative confocal micrographs of HeLa cells treated with nontargeting (siNT), siATG14L, or siUVRAG siRNAs that were infected with $DsRed_m$-expressing *B. abortus* 2308 (red) for 72 hr pi and processed for LAMP-1 immunostaining (blue). Quantification of aBCV formation (middle) in HeLa cells treated with nontargeting (siNT), siATG14L, or siUVRAG siRNAs and infected with $DsRed_m$-expressing *B. abortus* 2308 (red) for 24, 48 or 72 hr is shown. Data are shown as means ± SD from three independent experiments. Asterisks denote statistically significant differences (two-tailed Student's t test; $p < 0.05$).

See also Figure S5.

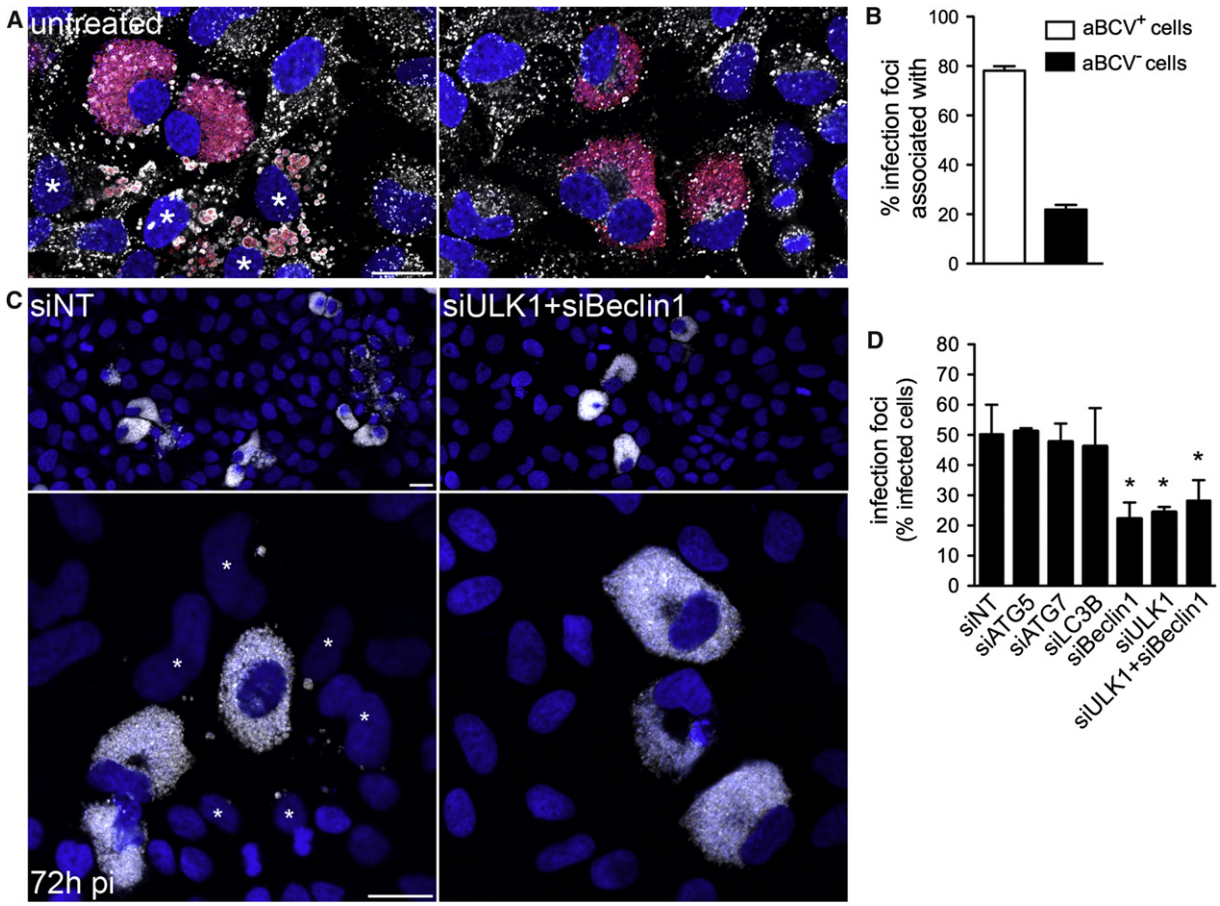

Figure 6. aBCV Formation Promotes Reinfection Events

(A) Representative confocal micrographs of HeLa cells infected with $DsRed_m$-expressing *B. abortus* 2308, incubated under reinfection-permissive conditions for 24 hr before analysis at 72 hr pi, and immunostained for LAMP-1 to detect aBCVs. Asterisks denote reinfected cells neighboring a primary infected cell containing aBCVs (left). Infected cells that do not contain aBCVs (right) are not associated with infection foci. Bacteria are shown in red, LAMP-1 is pseudocolored in white, and DNA is shown in blue.

(B) Association of aBCV-containing cells with infection foci. Infection foci were examined for their association with aBCV-containing cells at 72 hr pi. Data are shown as means ± SD from three independent experiments.

(C) Representative confocal micrographs of HeLa cells treated with either nontargeting (siNT; left) or siULK1+siBeclin1 siRNA (right) infected with $DsRed_m$-expressing *B. abortus* 2308 (pseudocolored in white), incubated under reinfection-permissive conditions for 24 hr before analysis at 72 hr pi and stained for DAPI (shown in blue). Asterisks denote reinfected cells. Scale bars represent 20 μm.

(D) Quantification of infection foci at 72 hr pi in HeLa cells treated with nontargeting (siNT), siATG5, siATG7, siLC3B, siBeclin1, siULK1, or siULK1+siBeclin1 siRNAs. Data are shown as means ± SD from three independent experiments. Asterisk denotes a statistically significant difference from the siNT control (two-tailed Student's t test; $p < 0.05$).

See also Figure S6.

Reagents

Antibodies used for immunofluorescence microscopy were as follows: rat anti-mouse LAMP-1 (clone 1D4B, developed by J.T. August and obtained from the Developmental Studies Hybridoma Bank [DSHB] developed under the auspices of the National Institute of Child Health and Human Development and maintained by The University of Iowa, Department of Biological Sciences, Iowa City, IA), mouse anti-human LAMP-1 (clone H4A3, DSHB), rabbit monoclonal anti-Rab7 (clone D95F2, Cell Signaling Technology, Boston, MA), mouse anti-LC3A/B (Clone 4E12; Medical and Biological Laboratories [MBL], Japan), rabbit polyclonal anti-LC3A/B/C (MBL), rabbit polyclonal anti-calnexin (Assay Designs, Ann Arbor, MI), rabbit polyclonal anti-calreticulin (Affinity BioReagents, Golden, CO), and Alexa Fluor 488-donkey anti-mouse, anti-rat, or Cyanin 5-conjugated goat anti-rabbit, anti-mouse (Jackson ImmunoResearch Laboratories, West Grove, PA). Rabbit polyclonal anti-actin (Bethyl Laboratories, Montogomery, TX), mouse monoclonal anti-GAPDH (Affinity Bioreagents, Rockford, IL), rabbit polyclonal anti-ATG5 (Cell Signaling Technology), rabbit anti-ULK1(R600) (Cell Signaling Technology), rabbit anti-LC3B(D11)XP (Cell Signaling Technology), rabbit anti-ATG7 (Cell Signaling Technology), mouse monoclonal anti-Beclin1 (Abgent, San Diego, CA), rabbit anti-ATG14L (MBL), rabbit anti-UVRAG (Matsunaga et al., 2009), and HRP-conjugated anti-rabbit IgG or anti-mouse IgG (1:10,000, Cell Signaling Technology) were used for western blotting. DAPI and propidium iodide (Invitrogen, Carlsbad, CA) were used as DNA stains. siRNA-mediated knockdown of mammalian proteins was performed using ON-TARGETplus SMARTpool siRNA (Thermo Fisher Scientific, Lafayette, CO) and ON-TARGETplus Non-Targeting Pool siRNA (D-001810) as control. siRNA against human proteins included ATG5 (L-004374), LC3B (L-012846), ATG7 (L-020112), Beclin1 (L-010552), ULK1 (L-005049), ATG14L (KIAA0831, L-020438), and UVRAG (L-015465), and mouse proteins included Atg7 (L-049953) and Beclin1 (L-055895).

Cell Culture, Infections, and Determination of Bacterial CFUs

BMMs from C57BL/6J (Jackson Laboratories, Bar Harbor, ME), *Atg5*$^{flox/flox}$ and *Atg5*$^{flox/flox}$-*lyz-Cre* (Zhao et al., 2008), *Atg16L1*$^{flox/flox}$ and *Atg16L1*$^{flox/flox}$-*lyz-Cre* (H.W.V. and S.H., unpublished data), or *Atg4B*$^{-/-}$ mice (Mariño et al., 2010) were harvested according to procedures approved by the Rocky Mountain Laboratories Animal Care and Use Committee and processed as described (Chong et al., 2008). HeLa cells (ATCC clone CCL-2) were cultured as described (Starr et al., 2008). For infections, cells were seeded either on 12 mm glass coverslips in 24-well plates (for microscopy; 5 × 10^4/well) or 6-well plates (for western blot analysis; 1.5 × 10^5/well) 24 to 48 hr prior to infection. Infections were performed as described (Starr et al., 2008), except that cells were maintained in gentamicin-free medium until 24 hr, then afterwards in medium containing 25 μg/ml gentamicin to prevent reinfection events, unless specified otherwise. In reinfection experiments, gentamicin was removed at 48 hr pi from infected HeLa cells and samples processed at 72 hr pi and analyzed for infection foci. These were defined as a cell containing high numbers of bacteria (primary infection) surrounded by at least four adjacent cells containing few bacteria (secondary infection). For inhibition of PI3-kinase activity, BMMs and HeLa cells were incubated with 3-methyladenine (3-MA) (Sigma, St. Louis, MO; 10 mM) or LY294002 (Cell Signaling Technology; 50 μM) for 16 hr prior to analysis, without any detectable cytotoxicity. For labeling of acidic compartments, BMMs were incubated in presence of 50 nM LysoTracker Red DND-99 (Invitrogen) for 1 hr prior to analysis. For labeling of the endocytic compartment, BMMs were incubated in presence of 50 μg/ml Alexa Fluor 568-conjugated dextran (MW10,000; Invitrogen) for 2 hr and immediately analyzed by confocal live-cell imaging. For evaluation of intracellular growth, the number of viable intracellular bacteria per well was determined for each time point through enumeration of colony forming units (CFUs) as described (Starr et al., 2008).

Transfections and siRNA-Mediated Depletion of Host Proteins

A plasmid expressing 2xFYVE-EGFP (pEGFP-2xFYVE, a gift from George Banting [Pattni et al., 2001]) was transfected in HeLa cells 1 day prior to infection using FuGene6 transfection reagent (Roche) according to the manufacturer's instructions. For siRNA-mediated depletion, HeLa cells were transfected 24 hr prior to infection using DharmaFECT1 Transfection Reagent (Dharmacon) with 30–100 nM siRNA. BMMs (1.5 × 10^6 cells) were transfected via nucleofection with 2 μM of siRNA using the Amaxa Biosystems Mouse Macrophage Nucleofector kit (Lonza, Basel, Switzerland) and a Nucleofector II electroporator (program Y-001) 16 hr prior to infection. After nucleofection, cells were plated at 5 × 10^4 cells/well (24-well plate) or 4 × 10^5 cells/well (12-well plate). Protein depletion was verified at times equivalent to 0 and 72 hr pi by western blotting and densitometry analysis with a Kodak Image Station 4000MM PRO (Eastmann Kodak, Rochester NY).

Microscopy

For immunofluorescence microscopy, infected cells were processed as described (Starr et al., 2008), and samples were observed on a Carl Zeiss AxioImager epi-fluorescence microscope equipped with a Plan Apo 63×/1.4 objective for quantitative analysis or a Carl Zeiss LSM 710 confocal laser scanning microscope for image acquisition (Carl Zeiss Micro Imaging, Thornwood, NY). Confocal images of 1024 × 1024 pixels were acquired with the Carl Zeiss ZEN 2008 software and assembled with Adobe Photoshop CS3 (Adobe Systems, San Jose, CA). Live-cell imaging analysis was performed on a Carl Zeiss MicroImaging LSM 5 LIVE confocal laser scanning microscope equipped with a LCI Plan 63×/1.45 NA objective. Images (768 × 768 pixels) were acquired with 488 nm and 561 nm solid-state lasers for sequential excitation and the Carl Zeiss ZEN 2008 software and were assembled in Adobe Photoshop CS3. Transmission electron microscopy (TEM) was performed as described in the Supplemental Experimental Procedures.

Western Blot Analysis

Samples were normalized to total protein concentrations, resolved on SDS-PAGE and transferred to Hybond-ECL nitrocellulose membranes (Amersham Biosciences) as described previously (Chong et al., 2008). Total protein concentration was determined using a BCA protein Assay Kit (Pierce).

Statistical Analysis

A Student's t test was used to assess statistical differences between two experimental data sets, while multiple comparisons were performed with a one-way ANOVA followed by a Tukey's test. All values shown, unless otherwise stated, are the mean values ± the SD from three independent experiments.

SUPPLEMENTAL INFORMATION

Supplemental Information includes Supplemental Experimental Procedures and six figures and can be found with this article online at doi:10.1016/j.chom.2011.12.002.

ACKNOWLEDGMENTS

We are grateful to Zijiang Zhao for his assistance in providing bone marrow from *ATG5*$^{flox/flox}$ and *ATG5*$^{flox/flox}$-*lyz-Cre* mice, and to George Banting, Joyce Karlinsey, Tamotsu Yoshimori, Ed Miao, and Leigh Knodler for providing reagents and helpful suggestions. We thank Bob Heinzen and Leigh Knodler for critical reading of the manuscript. This work was supported by the Intramural Research Program of the National Institutes of Health, National Institute of Allergy and Infectious Diseases, by grant U54 AI057160 to H.W.V., and by the Ministry of Science and Innovation, Spain, FP7 (Microenvimet) and the Botin Foundation to C.L.-O.

Received: June 10, 2011
Revised: October 26, 2011
Accepted: December 1, 2011
Published: January 18, 2012

REFERENCES

Archambaud, C., Salcedo, S.P., Lelouard, H., Devilard, E., de Bovis, B., Van Rooijen, N., Gorvel, J.P., and Malissen, B. (2010). Contrasting roles of macrophages and dendritic cells in controlling initial pulmonary Brucella infection. Eur. J. Immunol. *40*, 3458–3471.

Arellano-Reynoso, B., Lapaque, N., Salcedo, S., Briones, G., Ciocchini, A.E., Ugalde, R., Moreno, E., Moriyón, I., and Gorvel, J.P. (2005). Cyclic beta-1,2-glucan is a Brucella virulence factor required for intracellular survival. Nat. Immunol. *6*, 618–625.

Axe, E.L., Walker, S.A., Manifava, M., Chandra, P., Roderick, H.L., Habermann, A., Griffiths, G., and Ktistakis, N.T. (2008). Autophagosome formation from membrane compartments enriched in phosphatidylinositol 3-phosphate and dynamically connected to the endoplasmic reticulum. J. Cell Biol. *182*, 685–701.

Bellaire, B.H., Roop, R.M., 2nd, and Cardelli, J.A. (2005). Opsonized virulent Brucella abortus replicates within nonacidic, endoplasmic reticulum-negative, LAMP-1-positive phagosomes in human monocytes. Infect. Immun. *73*, 3702–3713.

Bernales, S., McDonald, K.L., and Walter, P. (2006). Autophagy counterbalances endoplasmic reticulum expansion during the unfolded protein response. PLoS Biol. *4*, e423.

Birmingham, C.L., Smith, A.C., Bakowski, M.A., Yoshimori, T., and Brumell, J.H. (2006). Autophagy controls Salmonella infection in response to damage to the Salmonella-containing vacuole. J. Biol. Chem. *281*, 11374–11383.

Birmingham, C.L., Canadien, V., Gouin, E., Troy, E.B., Yoshimori, T., Cossart, P., Higgins, D.E., and Brumell, J.H. (2007). Listeria monocytogenes evades killing by autophagy during colonization of host cells. Autophagy *3*, 442–451.

Boschiroli, M.L., Ouahrani-Bettache, S., Foulongne, V., Michaux-Charachon, S., Bourg, G., Allardet-Servent, A., Cazevieille, C., Liautard, J.P., Ramuz, M., and O'Callaghan, D. (2002). The Brucella suis virB operon is induced intracellularly in macrophages. Proc. Natl. Acad. Sci. USA *99*, 1544–1549.

Celli, J., de Chastellier, C., Franchini, D.-M., Pizarro-Cerda, J., Moreno, E., and Gorvel, J.P. (2003). Brucella evades macrophage killing via VirB-dependent sustained interactions with the endoplasmic reticulum. J. Exp. Med. *198*, 545–556.

Celli, J., Salcedo, S.P., and Gorvel, J.P. (2005). Brucella coopts the small GTPase Sar1 for intracellular replication. Proc. Natl. Acad. Sci. USA *102*, 1673–1678.

Checroun, C., Wehrly, T.D., Fischer, E.R., Hayes, S.F., and Celli, J. (2006). Autophagy-mediated reentry of Francisella tularensis into the endocytic compartment after cytoplasmic replication. Proc. Natl. Acad. Sci. USA *103*, 14578–14583.

Chong, A., Wehrly, T.D., Nair, V., Fischer, E.R., Barker, J.R., Klose, K.E., and Celli, J. (2008). The early phagosomal stage of Francisella tularensis determines optimal phagosomal escape and Francisella pathogenicity island protein expression. Infect. Immun. *76*, 5488–5499.

Collins, C.A., De Mazière, A., van Dijk, S., Carlsson, F., Klumperman, J., and Brown, E.J. (2009). Atg5-independent sequestration of ubiquitinated mycobacteria. PLoS Pathog. *5*, e1000430.

Comerci, D.J., Martínez-Lorenzo, M.J., Sieira, R., Gorvel, J.P., and Ugalde, R.A. (2001). Essential role of the VirB machinery in the maturation of the Brucella abortus-containing vacuole. Cell. Microbiol. *3*, 159–168.

de Jong, M.F., Sun, Y.H., den Hartigh, A.B., van Dijl, J.M., and Tsolis, R.M. (2008). Identification of VceA and VceC, two members of the VjbR regulon that are translocated into macrophages by the Brucella type IV secretion system. Mol. Microbiol. *70*, 1378–1396.

Dorn, B.R., Dunn, W.A., Jr., and Progulske-Fox, A. (2001). Porphyromonas gingivalis traffics to autophagosomes in human coronary artery endothelial cells. Infect. Immun. *69*, 5698–5708.

Ferrero, M.C., Fossati, C.A., and Baldi, P.C. (2009). Smooth Brucella strains invade and replicate in human lung epithelial cells without inducing cell death. Microbes Infect. *11*, 476–483.

Fugier, E., Salcedo, S.P., de Chastellier, C., Pophillat, M., Muller, A., Arce-Gorvel, V., Fourquet, P., and Gorvel, J.P. (2009). The glyceraldehyde-3-phosphate dehydrogenase and the small GTPase Rab 2 are crucial for Brucella replication. PLoS Pathog. *5*, e1000487.

Gross, A., Terraza, A., Ouahrani-Bettache, S., Liautard, J.P., and Dornand, J. (2000). In vitro Brucella suis infection prevents the programmed cell death of human monocytic cells. Infect. Immun. *68*, 342–351.

Gutierrez, M.G., Master, S.S., Singh, S.B., Taylor, G.A., Colombo, M.I., and Deretic, V. (2004). Autophagy is a defense mechanism inhibiting BCG and Mycobacterium tuberculosis survival in infected macrophages. Cell *119*, 753–766.

Gutierrez, M.G., Vázquez, C.L., Munafó, D.B., Zoppino, F.C., Berón, W., Rabinovitch, M., and Colombo, M.I. (2005). Autophagy induction favours the generation and maturation of the Coxiella-replicative vacuoles. Cell. Microbiol. *7*, 981–993.

He, C., and Klionsky, D.J. (2009). Regulation mechanisms and signaling pathways of autophagy. Annu. Rev. Genet. *43*, 67–93.

Itakura, E., and Mizushima, N. (2010). Characterization of autophagosome formation site by a hierarchical analysis of mammalian Atg proteins. Autophagy *6*, 764–776.

Itakura, E., Kishi, C., Inoue, K., and Mizushima, N. (2008). Beclin 1 forms two distinct phosphatidylinositol 3-kinase complexes with mammalian Atg14 and UVRAG. Mol. Biol. Cell *19*, 5360–5372.

Levine, B., Mizushima, N., and Virgin, H.W. (2011). Autophagy in immunity and inflammation. Nature *469*, 323–335.

Liang, C., Lee, J.S., Inn, K.S., Gack, M.U., Li, Q., Roberts, E.A., Vergne, I., Deretic, V., Feng, P., Akazawa, C., and Jung, J.U. (2008). Beclin1-binding UVRAG targets the class C Vps complex to coordinate autophagosome maturation and endocytic trafficking. Nat. Cell Biol. *10*, 776–787.

Marchesini, M.I., Herrmann, C.K., Salcedo, S.P., Gorvel, J.P., and Comerci, D.J. (2011). In search of Brucella abortus type IV secretion substrates: screening and identification of four proteins translocated into host cells through VirB system. Cell. Microbiol. *13*, 1261–1274.

Mariño, G., Fernández, A.F., Cabrera, S., Lundberg, Y.W., Cabanillas, R., Rodríguez, F., Salvador-Montoliu, N., Vega, J.A., Germanà, A., Fueyo, A., et al. (2010). Autophagy is essential for mouse sense of balance. J. Clin. Invest. *120*, 2331–2344.

Matsunaga, K., Saitoh, T., Tabata, K., Omori, H., Satoh, T., Kurotori, N., Maejima, I., Shirahama-Noda, K., Ichimura, T., Isobe, T., et al. (2009). Two Beclin 1-binding proteins, Atg14L and Rubicon, reciprocally regulate autophagy at different stages. Nat. Cell Biol. *11*, 385–396.

Matsunaga, K., Morita, E., Saitoh, T., Akira, S., Ktistakis, N.T., Izumi, T., Noda, T., and Yoshimori, T. (2010). Autophagy requires endoplasmic reticulum targeting of the PI3-kinase complex via Atg14L. J. Cell Biol. *190*, 511–521.

Mizushima, N., Yoshimori, T., and Levine, B. (2010). Methods in mammalian autophagy research. Cell *140*, 313–326.

Moreau, K., Lacas-Gervais, S., Fujita, N., Sebbane, F., Yoshimori, T., Simonet, M., and Lafont, F. (2010). Autophagosomes can support Yersinia pseudotuberculosis replication in macrophages. Cell. Microbiol. *12*, 1108–1123.

Nakagawa, I., Amano, A., Mizushima, N., Yamamoto, A., Yamaguchi, H., Kamimoto, T., Nara, A., Funao, J., Nakata, M., Tsuda, K., et al. (2004). Autophagy defends cells against invading group A Streptococcus. Science *306*, 1037–1040.

Nishida, Y., Arakawa, S., Fujitani, K., Yamaguchi, H., Mizuta, T., Kanaseki, T., Komatsu, M., Otsu, K., Tsujimoto, Y., and Shimizu, S. (2009). Discovery of Atg5/Atg7-independent alternative macroautophagy. Nature *461*, 654–658.

Ogata, M., Hino, S., Saito, A., Morikawa, K., Kondo, S., Kanemoto, S., Murakami, T., Taniguchi, M., Tanii, I., Yoshinaga, K., et al. (2006). Autophagy is activated for cell survival after endoplasmic reticulum stress. Mol. Cell. Biol. *26*, 9220–9231.

Ogawa, M., Yoshimori, T., Suzuki, T., Sagara, H., Mizushima, N., and Sasakawa, C. (2005). Escape of intracellular Shigella from autophagy. Science *307*, 727–731.

Pappas, G., Akritidis, N., Bosilkovski, M., and Tsianos, E. (2005). Brucellosis. N. Engl. J. Med. *352*, 2325–2336.

Pattni, K., Jepson, M., Stenmark, H., and Banting, G. (2001). A PtdIns(3)P-specific probe cycles on and off host cell membranes during Salmonella invasion of mammalian cells. Curr. Biol. *11*, 1636–1642.

Pizarro-Cerdá, J., Méresse, S., Parton, R.G., van der Goot, G., Sola-Landa, A., Lopez-Goñi, I., Moreno, E., and Gorvel, J.P. (1998a). Brucella abortus transits through the autophagic pathway and replicates in the endoplasmic reticulum of nonprofessional phagocytes. Infect. Immun. *66*, 5711–5724.

Pizarro-Cerdá, J., Moreno, E., Sanguedolce, V., Mege, J.L., and Gorvel, J.P. (1998b). Virulent Brucella abortus prevents lysosome fusion and is distributed within autophagosome-like compartments. Infect. Immun. *66*, 2387–2392.

Pujol, C., Klein, K.A., Romanov, G.A., Palmer, L.E., Cirota, C., Zhao, Z., and Bliska, J.B. (2009). Yersinia pestis can reside in autophagosomes and avoid xenophagy in murine macrophages by preventing vacuole acidification. Infect. Immun. *77*, 2251–2261.

Qin, Q.M., Pei, J., Ancona, V., Shaw, B.D., Ficht, T.A., and de Figueiredo, P. (2008). RNAi screen of endoplasmic reticulum-associated host factors reveals a role for IRE1alpha in supporting Brucella replication. PLoS Pathog. *4*, e1000110.

Rich, K.A., Burkett, C., and Webster, P. (2003). Cytoplasmic bacteria can be targets for autophagy. Cell. Microbiol. *5*, 455–468.

Salcedo, S.P., Marchesini, M.I., Lelouard, H., Fugier, E., Jolly, G., Balor, S., Muller, A., Lapaque, N., Demaria, O., Alexopoulou, L., et al. (2008). Brucella control of dendritic cell maturation is dependent on the TIR-containing protein Btp1. PLoS Pathog. *4*, e21.

Starr, T., Ng, T.W., Wehrly, T.D., Knodler, L.A., and Celli, J. (2008). Brucella intracellular replication requires trafficking through the late endosomal/lysosomal compartment. Traffic *9*, 678–694.

Sturgill-Koszycki, S., and Swanson, M.S. (2000). Legionella pneumophila replication vacuoles mature into acidic, endocytic organelles. J. Exp. Med. *192*, 1261–1272.

Sun, Q., Fan, W., Chen, K., Ding, X., Chen, S., and Zhong, Q. (2008). Identification of Barkor as a mammalian autophagy-specific factor for Beclin 1 and class III phosphatidylinositol 3-kinase. Proc. Natl. Acad. Sci. USA *105*, 19211–19216.

Swanson, M.S., and Isberg, R.R. (1995). Association of Legionella pneumophila with the macrophage endoplasmic reticulum. Infect. Immun. *63*, 3609–3620.

Thoresen, S.B., Pedersen, N.M., Liestøl, K., and Stenmark, H. (2010). A phosphatidylinositol 3-kinase class III sub-complex containing VPS15, VPS34, Beclin 1, UVRAG and BIF-1 regulates cytokinesis and degradative endocytic traffic. Exp. Cell Res. *316*, 3368–3378.

Yoshikawa, Y., Ogawa, M., Hain, T., Yoshida, M., Fukumatsu, M., Kim, M., Mimuro, H., Nakagawa, I., Yanagawa, T., Ishii, T., et al. (2009). Listeria monocytogenes ActA-mediated escape from autophagic recognition. Nat. Cell Biol. *11*, 1233–1240.

Zhao, Z., Fux, B., Goodwin, M., Dunay, I.R., Strong, D., Miller, B.C., Cadwell, K., Delgado, M.A., Ponpuak, M., Green, K.G., et al. (2008). Autophagosome-independent essential function for the autophagy protein Atg5 in cellular immunity to intracellular pathogens. Cell Host Microbe *4*, 458–469.

Zheng, Y.T., Shahnazari, S., Brech, A., Lamark, T., Johansen, T., and Brumell, J.H. (2009). The adaptor protein p62/SQSTM1 targets invading bacteria to the autophagy pathway. J. Immunol. *183*, 5909–5916.

Zhong, Y., Wang, Q.J., Li, X., Yan, Y., Backer, J.M., Chait, B.T., Heintz, N., and Yue, Z. (2009). Distinct regulation of autophagic activity by Atg14L and Rubicon associated with Beclin 1-phosphatidylinositol-3-kinase complex. Nat. Cell Biol. *11*, 468–476.